Recognition Elements for 5′ Exon Substrate Binding to the *Candida albicans* Group I Intron†

Matthew D. Disney,‡ Constantine G. Haidaris,§ and Douglas H. Turner*,‡,||

Departments of Chemistry, Pediatrics, and Microbiology and Immunology, University of Rochester, Rochester, New York 14627-0216

Received August 24, 2000; Revised Manuscript Received January 17, 2001

ABSTRACT: A group I intron precursor and ribozyme were cloned from the large subunit rRNA of the human pathogen *Candida albicans*. Both the precursor and ribozyme are functional as determined from in vitro assays. Comparisons of dissociation constants for oligonucleotide binding to the ribozyme and to a hexanucleotide mimic of its internal guide sequence lead to a model for recognition of the 5′ exon substrate by this intron. In particular, tertiary contacts with the P1 helix that help align the splice site include three 2′-hydroxyl groups, a G·U pair that occurs at the intron's splice junction, and a G·A pair. The free energy contribution that each interaction contributes to tertiary binding is determined. When the G·A pair is replaced with a G-C pair, tertiary interactions to 5′ exon mimic 2′-hydroxyl groups are significantly weakened. When the G·A pair is replaced with a G·U pair, tertiary interactions are retained and binding is 10-fold tighter. These results expand our knowledge of substrate recognition by group I introns, and also provide a basis for rational design of oligonucleotide-based therapeutics for targeting group I introns by binding enhancement by tertiary interactions and suicide inhibition strategies.

Candida albicans is a fungal pathogen that poses a serious risk to the health of immunocompromised hosts, including AIDS patients, cancer patients, diabetics, and newborns. Furthermore, this fungus is responsible for 8% of all hospital-acquired infections (*1*). Current treatments against *C. albicans*, however, are losing their efficacy because fungi are evolving resistance to commonly used antifungal drugs (*2*). Group I introns are potential drug targets for combating *C. albicans* and other infections (*3*−*11*). Two approaches to targeting group I introns with oligonucleotide-based compounds are binding enhancement by tertiary interactions (BETI)[1] and suicide inhibition (*6*−*11*).

BETI is a strategy that takes advantage of tertiary interactions with a helix formed by an oligonucleotide and the RNA target and allows oligonucleotides to bind to the target with a much higher affinity and specificity than could be obtained by base pairing alone. Suicide inhibition is a means of targeting catalytic RNAs. In group I intron self-splicing, the intron recognizes the 3′ end of the flanking 5′ exon and ligates it to the 3′ exon. Suicide inhibition tricks the intron into ligating an oligonucleotide 5′ exon mimic to the 3′ exon (*9*), preventing formation of mature functional RNA.

BETI and suicide inhibition strategies have been demonstrated with a group I intron from the opportunistic fungus *Pneumocystis carinii* (*6*−*11*). Because *C. albicans* is more readily manipulated in cell cultures than *P. carinii* (*12*), it provides a more convenient system for testing RNA targeting strategies in vivo. To provide a foundation for the rational design of oligonucleotides for inhibiting group I intron self-splicing in *C. albicans*, this paper identifies contacts that are used to align the 5′ splice site for reaction. The results indicate that at least five contacts contribute to tertiary interactions with the intron: three 2′-hydroxyl groups, a G·U pair at the splice junction, and a G·A pair that is formed when the 5′ exon binds to the internal guide sequence (IGS) of the intron. The results reveal both similarities and differences with respect to the molecular recognition used by other group I introns.

MATERIALS AND METHODS

Buffers. H*X*Mg buffer is 50 mM Hepes (25 mM NaHepes), 135 mM KCl, and *X* mM $MgCl_2$ at pH 7.5. M10Mg buffer is 50 mM Mes (25 mM NaMes), 135 mM KCl, and 10 mM $MgCl_2$ at pH 6.5. TBE buffer is 100 mM Tris, 90 mM boric acid, and 1 mM EDTA at pH 8.4. Stop buffer contains 8 M urea, 12 mM Na_2EDTA, and 0.1× TBE buffer. The 2 M TEAA buffer was made by adding reagent grade triethylamine to a solution containing 2 M glacial acetic acid until the pH reached 7.5. The 3′ end reaction buffer is 20 mM Tris-HCl (pH 7.0), 50 mM KCl, 700 μM $MnCl_2$, 200 μM EDTA, 100 μg/mL BSA, and 10% glycerol.

† This work was supported by NIH Grant AI45398. M.D.D. was partially supported by an Elon Huntington Hooker fellowship.

* To whom correspondence should be addressed. Phone: (716) 275-3207. Fax: (716) 473-6889. E-mail: Turner@chem.rochester.edu.

‡ Department of Chemistry.

§ Department of Microbiology and Immunology.

|| Department of Pediatrics.

[1] Abbreviations: BETI, binding enhancement by tertiary interactions; BSA, bovine serum albumin; DTT, dithiothreitol; EDTA, ethylenediaminetetraacetic acid; Hepes, *N*-(2-hydroxyethyl)piperazine-*N*-2-ethanesulfonic acid; HPLC, high-performance liquid chromatography; IGS, internal guide sequence; K_M^{pG}, Michaelis−Menten constant for pG addition to the precursor; K_M^{pG}, Michaelis−Menten constant for pG addition catalyzed by the ribozyme; LSU, large subunit; Mes, 2-(*N*-morpholino)ethanesulfonic acid; NTPs, nucleotide triphosphates; PAGE, polyacrylamide gel electrophoresis; rRNA, ribosomal ribonucleic acid; TLC, thin-layer chromatography; T_m, melting temperature in degrees Celsius; T_M, melting temperature in kelvin; Tris, tris(hydroxymethyl)-aminomethane; YPD, yeast extract peptone dextrose.

10.1021/bi002008r CCC: $20.00
Published on Web 05/03/2001

Instruments and General Protocols. Optical melting experiments were performed on a Gilford 250 UV−vis spectrophotometer equipped with a model 2527 temperature programmer. Oligonucleotides were synthesized on an Applied Biosystems 392 solid-phase synthesizer using standard phosphoramidite chemistry (*13*) with monomers purchased from Glen Research (Baltimore, MD). All HPLC chromatographs were obtained on a Hewlett-Packard Series 1100 HPLC system with an attached UV−vis detector sampling at 254 nm. Analytical gels that contained less than 10% polyacrylamide were placed on chromatography paper and dried in a gel drier. Gels that contained ≥10% polyacrylamide were placed on film. Nondenaturing gels for all gel binding assays consisted of 10% polyacrylamide, and were prepared, run, and electrophoresed in H10Mg buffer at 37 °C. All radioactivity was quantified on a Molecular Dynamics phosphorimager with ImageQuaNT version 4.1 software.

Synthesis, Purification, and Labeling of Oligonucleotides. The PCR primers and other DNAs were synthesized trityl-on and purified as previously described (*11*). The RNA oligonucleotides were synthesized, deprotected, and purified as previously described (*11*, *14*−*16*). The purity of the RNA and RNA−DNA chimera oligonucleotides was confirmed by HPLC; all oligonucleotides were at least 95% pure. Oligonucleotides were 5′ end labeled with T4 kinase and [γ-^{32}P]ATP or 3′ end labeled via addition of [γ-^{32}P]-3′-deoxyadenosine (cordycepin) with yeast poly(A) polymerase as described previously (*10*, *11*).

Identification of C. albicans Strains Containing a Group I Intron in their LSU rRNA. C. albicans clinical isolates (obtained from the University of Rochester Medical Center, Rochester, NY) were grown overnight in YPD medium, and total cellular DNA was isolated via a Yeast Star DNA kit (Zymo Research, Orange, CA) using the standard protocol. The total DNA was used as a template in PCRs to identify intron-containing strains. Products were obtained using the primers d(GATCAACTTAGAACTGGTACGG) and d(GATAGTAGATAGGGACAGTG), which flank the region of the rDNA where the intron resides (*5*, *17*). Reactions yielded one of two products, an ∼200 or ∼600 bp band corresponding to isolates not containing or containing the intron, respectively.

The ∼600 bp PCR product was cloned into a TOPO/TA vector (Invitrogen) using the manufacturer's protocol. The resulting plasmid was transformed into *Escherichia coli* cells (*18*), harvested with a Qiagen Mini spin kit, and sequenced in both directions with T7 and SP6 primers with big dye chemistry (CORE Sequencing Lab, University of Rochester Medical Center).

Cloning of C-h and the C-10/1x Ribozyme. The truncated rRNA precursor, C-h, which contains the group I intron and truncated 5′ and 3′ exons, was PCR amplified from the TOPO/TA precursor plasmid with PCR primers d(GAATTCGGGTAAACGGCGGGAGTAAC) and d(ATTTAGGTGACACTATAG), which contain *Eco*RI and *Hin*dIII restriction sites on the 5′ and 3′ ends, respectively. The amplified product was digested with *Eco*RI and *Hin*dIII, purified on an agarose gel, and ligated into a pGEM-3zf(+) vector (Gibco). The plasmid was transformed, isolated, and sequenced as described above.

The C-10/1x ribozyme was derived from the *C. albicans* group I intron. This construct lacks both the 5′ and 3′ exons, as well as the first 10 nucleotides on the 5′ end and one nucleotide on the 3′ end of the intron. It was used to study the binding and reactivity of exogenous exon mimics. A pGEM-9zf(−) vector was used to construct the ribozyme because the vector's T7 promoter can be removed by digestion with *Sfi*I and *Xba*I. To control the transcription start position, a T7 promoter was placed directly upstream of the sense PCR primer used to amplify the construct. This new promoter was engineered such that transcription starts precisely at the beginning of the ribozyme. The ribozyme was PCR amplified from the TOPO/TA vector using primers d(AAAGGCCAAGTCGGCCTCTATACGACTCACTATAGGGAGGCAAAAGTAGGGACG), which contains both a 5′ *Sfi*I restriction site and a T7 promoter, and d(AAAATCTAGATTGCTCCAAGAAATCGCTTTCTC), which contains a *Xba*I restriction site. The amplified product was digested with *Sfi*I and *Xba*I and ligated into a pGEM-9zf(−) vector (Gibco).

Ribozyme and Precursor Synthesis. The C-10/1x plasmid was cut with *Xba*I, extracted with phenol and chloroform, ethanol precipitated, resuspended in sterile H_2O, and stored at −20 °C. Transcriptions containing 10 μg of the linearized plasmid were incubated for 1 h at 37 °C in 1 mL of 40 mM Tris-HCl, 12 mM $MgCl_2$, 10 mM DTT, 4 mM spermidine, and NTPs (1 mM each), with the pH adjusted to 7.5 before addition of 2000 units of T7 RNA polymerase. Then 100 units of RNase-free DNase was added to the reaction mixture and the mixture incubated for 20 min at 37 °C to digest the plasmid DNA. The mixture was extracted with phenol and chloroform and ethanol precipitated. The product was further desalted by size exclusion chromatography on a Sephadex G-10 column or by dialysis with sterile water. Fractions that contained RNA were pooled, ethanol precipitated, resuspended in sterile H_2O, and stored at −20 °C. The concentration of RNA was determined by UV absorbance at 70 °C using an extinction coefficient of 3.72×10^6 M^{-1} cm^{-1} at 260 nm, which was calculated on the basis of the nearest-neighbor method (*19*).

The C-h precursor plasmid was cut with *Hin*dIII, extracted, and precipitated as described above. The internally labeled precursor was synthesized with a Maxiscript T7 transcription kit (Ambion). After transcription, the unincorporated [γ-^{32}P]-ATP was removed via a Chromaspin 10 column (Clontech) and the reaction mixture purified on a 5% polyacrylamide gel. The precursor was removed from the gel via the crush and soak method (spinning with a sterile stir bar), concentrated with 2-butanol, ethanol precipitated, resuspended in sterile water, and stored at −20 °C.

Ribozyme and Precursor Kinetics. The C-h precursor was reannealed in H10Mg buffer by heating it at 55 °C for 5 min, placing it at room temperature for 1 min, and incubating it at 37 °C. Reactions were initiated by addition of a solution containing serially diluted pG in H10Mg buffer at 37 °C. At the appropriate time, a 4 μL aliquot of the reaction mixture was removed and placed in 4 μL of stop buffer. Reaction products were separated on a 5% polyacrylamide, 8 M urea gel. The radioactivity in each band was quantified by a Molecular Dynamics phosphorimager and corrected for the number of adenines in each product. The rate of reaction was determined either by fitting the fraction of reaction products as a function of time to a single exponential or by fitting the linear portion, usually the first 30% conversion,

of the time course to the pseudo-first-order rate equation:

$$k_{obs}t = \ln\left(1 - \frac{F_t}{F_\infty}\right) \quad (1)$$

where F_t is the fraction of the 5′ exon−3′ exon product at time t and F_∞ is the fraction of the 5′ exon−3′ exon product formed at 120 min. A plot of k_{obs} versus pG concentration was fit to the Michaelis−Menten equation:

$$k_{obs} = \frac{k_{cat}[R]_o[S]_o}{K_M + [S]_o} \quad (2)$$

where $[R]_o$ is the concentration of the RNA enzyme, $[S]_o$ is the concentration of the substrate, and K_M is the Michaelis−Menten constant. The data were fit by nonlinear least squares to the optimal values of K_M and k_{cat}.

The ribozyme's ability to catalyze the hydrolysis (*20*), pG addition (*21*), and exon ligation reactions (*22*) was also analyzed kinetically. Reactions designed to measure k_{cat} and K_M for the 5′ exon mimic, r(GACUCUCAA), in both the hydrolysis and the pG addition reactions did not fit a Michaelis−Menten mechanism. The k_{cat}/K_m, however, was determined for the 5′ exon mimic in H10Mg buffer via single-turnover experiments (*20*) in which a solution of varying ribozyme concentrations, 1−80 nM, was added to an equal volume of a solution containing a limiting amount, ∼80 pM, of 5′ exon mimic labeled on either the 5′ or 3′ end. Reactions were carried out as described for self-splicing, except that 500 μM pG was included for assessment of pG addition. Products were separated on a 20% polyacrylamide, 8 M urea gel. Reaction rates were determined by fitting the first 30% conversion to eq 1. Plots of k_{obs} versus C-10/x concentration were linear, and linear least-squares analysis yields k_{cat}/K_M as the slope. Reactions were also completed with a 3′ end-labeled 5′ exon mimic to ensure that the experiments with pG monitored pG addition and those in the absence of pG monitored hydrolysis; no hydrolysis product was formed in the presence of pG. The k_{cat} for pG addition to extended substrates with the sequence r[G(A/C)CUCU**N**] was measured in a solution containing 3.0 μM C-10/1x, 2.5 mM pG, and a trace, ∼80 pM, of oligonucleotide substrate.

Multiple-turnover experiments were used to determine Michaelis−Menten parameters for the 3′ exon mimic, r(GCUUAA). Reactions were initiated by adding an equal volume of 400 nM C-10/1x, which was reannealed as previously described, to a solution containing 200 μM 5′ exon mimic, r(GACUCU), and varying amounts of r(GCUUAA) at 37 °C. Reactions were carried out and analyzed as described for hydrolysis, and Michaelis−Menten parameters were determined by fitting to eq 2.

Michaelis−Menten parameters for pG in pG addition to the 5′ exon mimic, r(GACUCUCAA), were also measured. In a typical experiment, 400 nM C-10/1x, reannealed as previously described, was added to an equal volume of a solution containing 200 μM 5′ exon mimic, r(GACUCUCAA), a trace amount of 5′-labeled r(GACUCUCAA) or 3′-end-labeled r(GACUCUCAAA), and a varying amount of pG, 0.4−4000 μM, at 37 °C.

Active-Site Titration. For a typical active-site titration (*23*, *24*), a limiting amount of C-10/1x (360 nM) was reannealed in H10Mg buffer. A second solution of equal volume containing 200 μM r(GCUUAA) and 2.5 μM r(GACUCU) with trace amounts of 5′-end-labeled r(GACUCU) in H10Mg buffer was added to the ribozyme solution at 37 °C. The first turnover in the reaction occurs at a rate $k_{forward}$, and subsequent turnovers occur at a rate k_{cat}. The size of the burst is given by eq 3 (*23*, *24*):

$$\pi = \left(\frac{k_{forward}}{k_{forward} + k_{release}}\right)^2 \frac{[R]_{active}}{[R]_o} \quad (3)$$

where $[R]_o$ is the total ribozyme concentration and $[R]_{active}$ is the concentration of the active ribozyme. The number of ribozyme turnovers, or [r(GACUCUCUUAA)]/$[R]_o$, versus time was plotted, and the burst, π, is equal to the fraction of active ribozyme when $k_{forward} \gg k_{release}$. The value of π was determined as the y-intercept of a linear least-squares line through the initial portion of the multiple-turnover region of the plot.

Gel Binding Assays. The ability of the C-10/1x ribozyme to bind the 5′ exon mimic, r(GACUCU), was determined by both direct and competitive gel binding assays. Due to subtle differences in the binding constants measured from different ribozyme preparations, comparisons are only made between measurements with the same preparation. In a typical direct binding assay (*6*, *9*, *25*, *26*), serially diluted concentrations of ribozyme were reannealed as described above in H10Mg buffer with 5% glycerol and added to ∼80 pM 5′-end-labeled 5′ exon mimic at 37 °C and incubated for at least 1 h. The bound species were separated by PAGE using H10Mg as the electrophoresis buffer, and the data were fit to the equation:

$$\Theta = \frac{[R]}{[R] + K_d} \quad (4)$$

where Θ is the fraction of r(GACUCU) bound to the ribozyme, [R] is the ribozyme concentration, and K_d is the ribozyme dissociation constant. The curves were fit by nonlinear least squares to the optimal value of K_d. A direct binding assay was also used to assess the binding of substrates extended beyond the splice site, r(GACUCU**N**). These experiments were completed in M10Mg buffer (pH 6.5) to minimize the amount of oligonucleotide hydrolyzed by the ribozyme; in each experiment, less than 5% hydrolysis was observed.

Competitive gel binding assays were used to analyze the binding of various substrates to the ribozyme. In these experiments, a solution containing 250 nM C-10/1x and 10% glycerol in H10Mg buffer was reannealed as described above and 5 μL added to 2 μL of a second solution containing trace 5′-end-labeled r(GACUCU) and serially diluted competitor oligonucleotide in H10Mg buffer at 37 °C. Reaction mixtures were incubated for at least 1 h and bound and unbound species separated by PAGE as described above. The fraction of 5′ exon mimic bound (Θ) as a function of added competitor was fit via nonlinear least squares to the equation (*10*, *11*, *26*−*28*)

$$\Theta = \frac{1}{2T_t}\left[K_t + \frac{K_t}{K_d}C_t + R_t + T_t - \sqrt{\left(K_t + \frac{K_t}{K_d}C_t + R_t + T_t\right)^2 - 4T_tR_t}\right] + A \quad (5)$$

where R_t, T_t, and C_t are the total concentrations of C-10/1x, radiolabeled r(GACUCU), and unlabeled competitor oligonucleotide, respectively, K_t is the dissociation constant for r(GACUCU) binding C-10/1x, determined from the direct gel binding assay, K_d is the competitor's dissociation constant, and A is the amount of radiolabel that is bound at infinite competitor concentration. The curves were fit by nonlinear least squares to the optimal values of A, K_d, and T_t.

Base Pairing to Mimics of the Intron's Internal Guide Sequence. The free energy of base pairing to mimics of the intron's internal guide sequence, r(GGAGGC), was either predicted via a nearest-neighbor analysis or measured by optical melting experiments. The free energies of r(GACUCU), r(_ACUCU), r(**U**GACUCU), and r(_**G**CUCU) binding to r(GGAGGC) were calculated from the measured values for r(GACUC**C**), r(_ACUC**C**), or r(_**G**CUC**C**) by adding the expected destabilization of 1.6 kcal/mol for changing the terminal G-C pair to a G·U pair; this includes a penalty of 0.45 kcal/mol if the duplex ends in a G·U or A·U pair (*29*−*31*). The free energy contribution of dangling ends or terminal noncanonical pairs on G·U pairs was estimated from the free energies on A-U pairs (*29*, *32*). All optical melting experiments were completed in H10Mg buffer and analyzed as described previously (*11*, *33*, *34*).

RESULTS

Secondary Structure. Figure 1 shows the sequence of the truncated precursor and the secondary structure of the *C. albicans* group I intron by analogy to the structure previously reported (*5*). The only difference in sequence with that previously reported is nucleotide 88, which is an A in Figure 1 instead of a C. Because of this difference in sequence, the P2.1 helix was folded with the program RNAstructure (*31*), to generate the predicted lowest-free energy folding shown in Figure 1.

Precursor Self-Splicing. The ability of the C-h precursor to self-splice in H10Mg buffer was examined as a function of pG concentration (Figure 2 and Table 1). Data were fit to a Michaelis−Menten mechanism as described by Bass and Cech (*35*). The precursor self-splices with K_M^{pG}, k_{cat}, and k_{cat}/K_M^{pG} values of 14 μM, 0.21 min^{-1}, and 15 $\times$ 10^3 M^{-1} min^{-1}, respectively, at 37 °C. As shown in Table 1, these parameters are similar to those determined for the *Tetrahymena thermophila* precursor at 30 °C (*35*).

Ribozyme Reaction Kinetics. The ability of the C-10/1x ribozyme to catalyze oligonucleotide ligation, pG addition, and hydrolysis reactions was analyzed in H10Mg buffer (Figure 3 and Table 2). For pG addition to r(GACUCUCAA), the Michaelis−Menten parameters K_M^{pG}, k_{cat}, and k_{cat}/K_M^{pG} are 166 μM, 0.57 min^{-1}, and 3.5 $\times$ 10^3 M^{-1} min^{-1}, respectively, similar to the parameters for the *T. thermophila* ribozyme (*20*). For the ligation of the 5′ exon mimic, r(GACUCU), with the 3′ exon mimic, r(GCUUAA), to yield r(GACUCUCUUAA), $K_M^{3'exon}$, k_{cat}, and $k_{cat}/K_M^{3'exon}$ are 0.87 μM, 0.39 min^{-1}, and 4.5 $\times$ 10^5 M^{-1} min^{-1}, respectively.

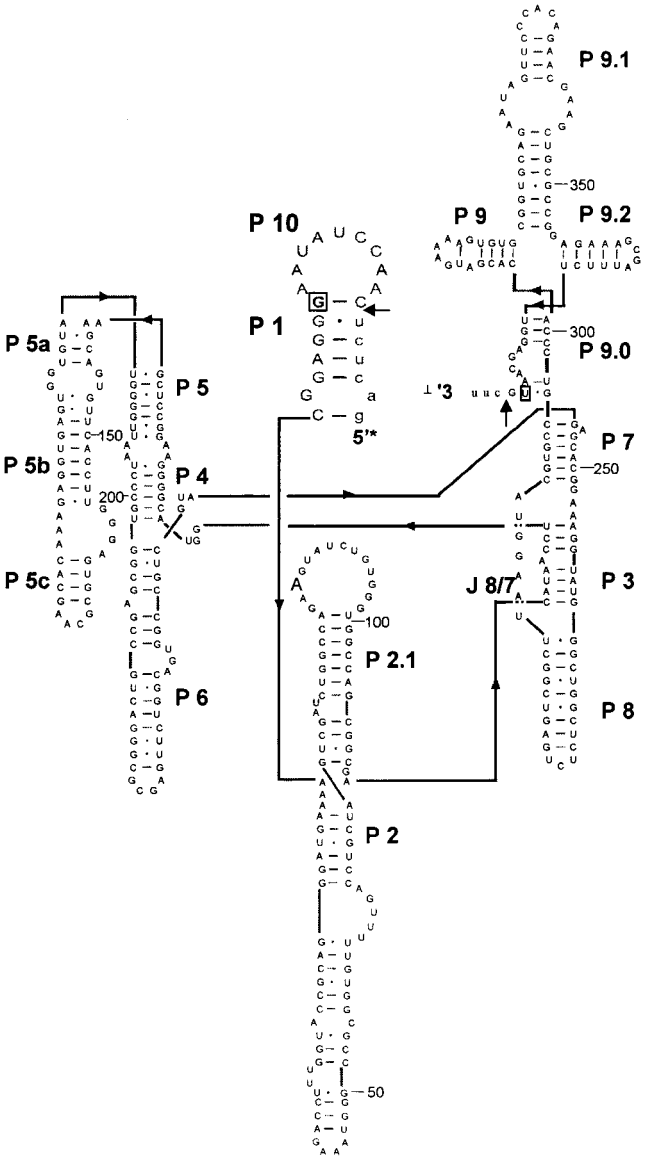

5′ **gggcgaattc**ggguaaacggcgggaguaacuau*3′

5′⊥ aaggtagccaaatgcctcgtcatctaattagtgacgcgcgcatgagtggattaacgagattcc cactgtccctatctatctactatca 3′

FIGURE 1: Secondary structure of the *C. albicans* group I intron from the large subunit rRNA with flanking 5′ and 3′ exon sequences for the truncated precursor construct. The structure is adapted from the previously reported secondary structure (*5*) with modifications in the P2.1 region due to the A88 (depicted in a larger font) versus C88 difference in sequence. The intron is depicted in uppercase letters, and the exons are depicted in lowercase letters. Arrows point to the 5′ and 3′ splice sites. The C-10/1x ribozyme starts at G11 and ends at U377 as indicated by boxed letters. The 5′ and 3′ exon nucleotides in bold are endogenous to the vector.

The k_{cat}/K_M values for r(GACUCUCAA) in the pG addition and hydrolysis reactions were measured via single-turnover experiments in the presence and absence, respectively, of excess, 500 μM, pG (Table 2). The k_{cat}/K_M values are 4.0 $\times$ 10^7 and 2.0 $\times$ 10^7 M^{-1} min^{-1}, respectively. Both are similar to values determined for the *T. thermophila* ribozyme using single-turnover measurements (*20*).

Active-Site Titration. An active-site titration was performed to determine the fraction of ribozyme that binds substrate and catalyzes the oligonucleotide ligation reaction in H10Mg buffer (Figure 4). Under experimental conditions of 180 nM C-10/1x, 100 μM r(GCUUAA), and 1.25 μM r(GACUCU)

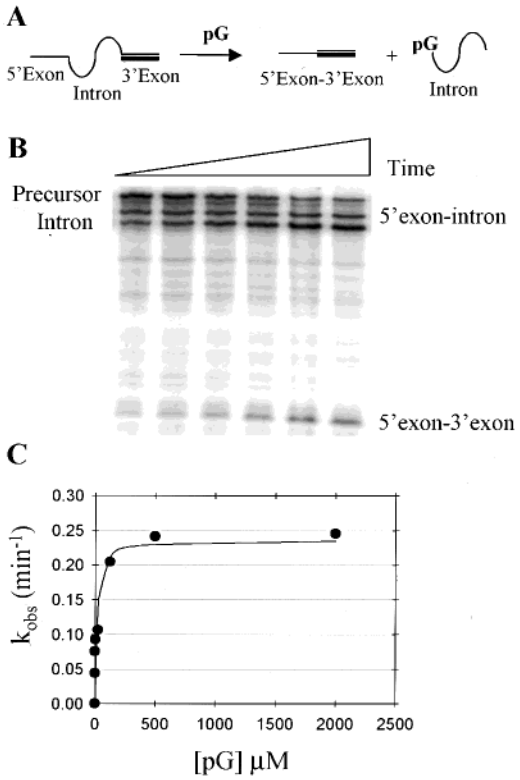

FIGURE 2: Self-splicing of the C-h precursor in H10Mg buffer. (A) The reaction scheme for precursor self-splicing. (B) An autoradiogram of a typical gel. (C) Fit of the data to a Michaelis−Menten mechanism.

Table 1: K_M^{pG}, k_{cat}, and k_{cat}/K_M^{pG} for Precursor Splicing

organism	K_M^{pG} (μM)	k_{cat} (min^{-1})	k_{cat}/K_M^{pG} (M^{-1} min^{-1})
C. albicans[a]	14	0.21	15×10^3
T. thermophilia[b]	20	0.52	25×10^3

[a] Reactions were carried out in H10Mg buffer at 37 °C and pH 7.5. Kinetic parameters were determined via a nonlinear least-squares fit to eq 2 by using the observed rate of reaction vs pG concentration (Figure 2). [b] These values were previously reported by Bass and Cech (*35*) and are for addition of guanosine at 30 °C.

in H10Mg buffer, a burst is observed, which suggests that $k_{forward} > k_{release}$ (see the reaction scheme in Figure 4). Extrapolating the size of the burst to the *y*-axis indicates that ~94% of the ribozyme is active in H10Mg buffer when reannealed as described in Materials and Methods.

Binding of 5′ Exon Mimic Substrates to C-10/1x and IGS Mimics. A competitive gel retardation assay (*6*, *26*, *27*) was used to assess binding to the C-10/lx ribozyme by oligonucleotides with sequences that mimic the 3′ end of the 5′ exon. The natural 5′ exon mimic, r(GACUCU), binds to the ribozyme with a K_d of 6.9 nM, which is similar to the K_d of 3.8 nM determined from a direct gel binding assay (Figure 5 and Table 3). To determine factors important for recognition of the 5′ exon mimic by the ribozyme, binding to ribozyme and to r(GGAGGC), a mimic of the IGS, was assessed for oligonucleotides of varying length and base composition (Tables 3 and 4).

Recognition of the Nucleotide at Position −5. The natural 5′ exon mimic, r(GACUCU), forms a G·A pair when bound to the ribozyme (Figure 1). To determine the importance of the G·A pair for overall binding, it was replaced with a G·G pair, r(G**G**CUCU), a G-C pair, r(G**C**CUCU), and a G·U pair, r(G**U**CUCU) (Table 3 and Figure 5). The oligonucleotide r(G**G**CUCU) binds to the ribozyme with an affinity similar to that of the natural sequence, r(GACUCU), 4.0 versus 6.9 nM, respectively. The oligonucleotides r(G**C**CUCU) and r(G**U**CUCU), however, bind more tightly than the natural 5′ exon mimic, with K_d values of 0.7 and 0.6 nM, respectively (Table 3).

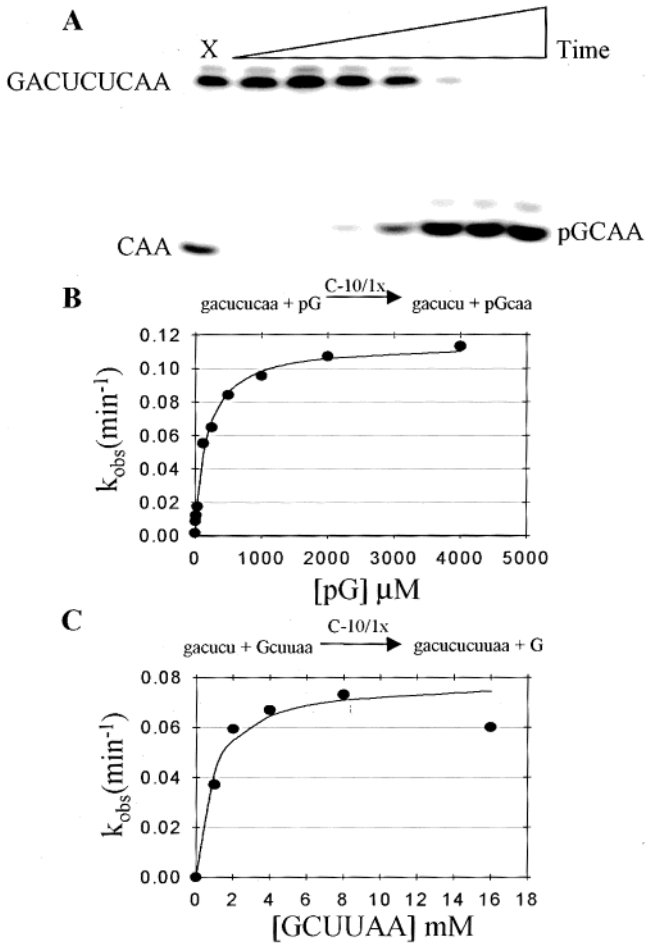

FIGURE 3: Cleavage and ligation reactions for the C-10/1x ribozyme. (A) An autoradiogram of a typical gel for the reaction of r(GACUCUCAA) with pG. Lane X represents a reaction in the absence of pG, and the lowest band is the hydrolysis product. (B) The reaction scheme for pG addition to the 5′ exon mimic, r(GACUCUCUU), and the data and curve fit for the reaction. (C) The reaction scheme for the oligonucleotide ligation reaction and the data and curve fit for the reaction.

Table 2: Kinetic Parameters for Reactions Catalyzed by C-10/1x (pG Addition, Exon Ligation, and Hydrolysis)[a]

reaction	5′ exon mimic	3′ exon mimic	K_M (μM)	k_{cat} (min^{-1})	k_{cat}/K_M (M^{-1} min^{-1})
pG addition[b]	GACUCUCAA	−	−	−	4.0×10^7
hydrolysis[b]	GACUCUCAA	−	−	−	2.0×10^7
pG addition[c]	GACUCUCAA	−	166	0.57	3.5×10^3
ligation[d]	GACUCU	GCUUAA	0.87[d]	0.39	4.5×10^5

[a] Kinetic parameters were determined by either single- or multiple-turnover experiments as described in Materials and Methods. All reactions were carried out in H10Mg buffer at 37 °C and pH 7.5. [b] The k_{cat}/K_M for GACUCUCAA was determined in single-turnover experiments via a linear least-squares fit to a plot of the reaction rate vs C-10/1x concentration. [c] The K_M^{pG}, k_{cat}, and k_{cat}/K_M^{pG} were determined from multiple-turnover experiments via a nonlinear least-squares fit to eq 2 by using the rate of reaction vs the pG concentration. [d] K_M for r(GCUUAA), the 3′ exon mimic, in the oligonucleotide ligation reaction.

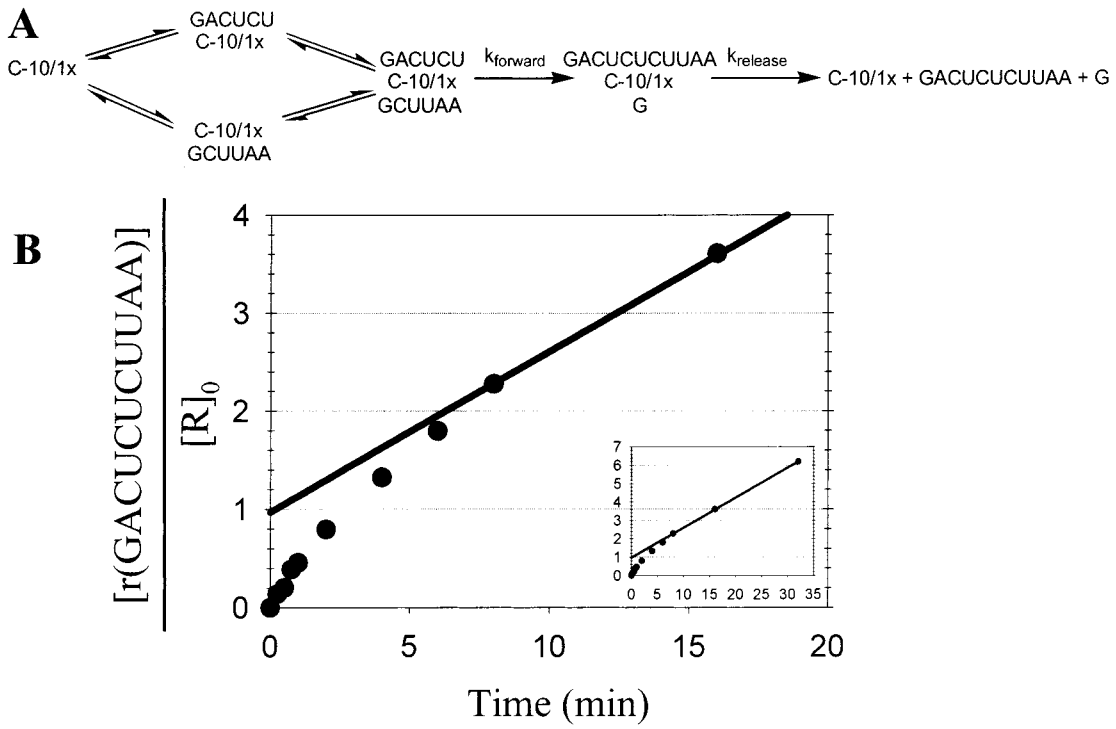

FIGURE 4: Active-site titration in H10Mg buffer to determine the fraction of active C-10/1x. (A) The reaction scheme for oligonucleotide ligation. (B) A plot of the number of ribozyme turnovers as a function of time. The straight line represents a fit by linear least squares to the initial part of the multiple-turnover portion of the curve. The burst, π, is the *y*-intercept of the line (*23*). The inset plot shows the data expanded to the 32 min reaction point.

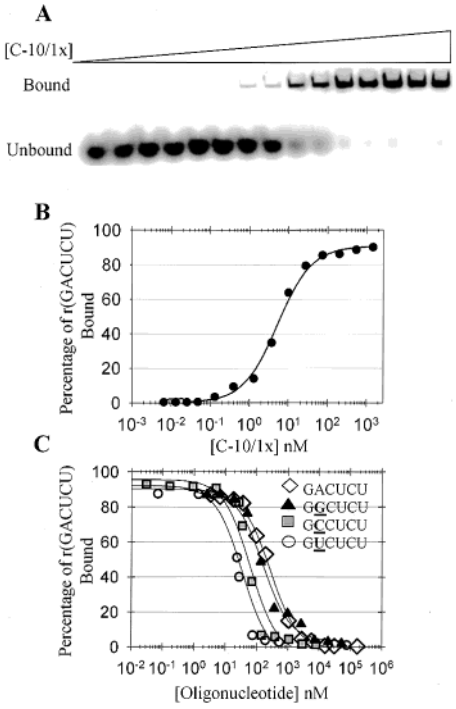

FIGURE 5: Binding assays for C-10/1x in H10Mg buffer. (A) An autoradiogram of a typical gel from a direct gel binding assay for r(GACUCU). (B) The data and curve fit from the above gel. (C) A competitive gel binding assay for r(GACUCU), r(G**G**CUCU), r(G**C**CUCU), and r(G**U**CUCU).

To partition overall binding into contributions from base pairing and tertiary interactions, stabilities of duplexes formed with the hexanucleotide r(GGAGGC) were either measured or predicted (Tables 3 and 4; see Materials and Methods for a description of the calculations). Both r(G**G**CUCU) and r(GACUCU) have similar contributions of base pairing and tertiary interactions to their overall binding affinity at 37 °C; base pairing contributes −4.1 and −4.2 kcal/mol for r(G-**G**CUCU) and r(GACUCU), respectively, and tertiary interactions contribute −7.8 and −7.4 kcal/mol for r(G**G**CUCU) and r(GACUCU), respectively (Tables 3 and 4). In contrast, the contributions of base pairing and tertiary interactions to the overall $\Delta G°$ of binding for r(G**C**CUCU) at 37 °C are −8.5 and −4.5 kcal/mol, respectively (Table 3). These results indicate that r(G**C**CUCU) binds more tightly to the ribozyme than r(GACUCU) because the increased level of base pairing of r(G**C**CUCU) more than compensates for the 2.9 kcal/mol weaker tertiary interactions.

Recognition of the Nucleotide at Position −1. The effect of changing the 3′ terminal U of the 5′ exon mimic to a C was investigated (Table 3). Similar experiments suggest that such a change provides an estimate of tertiary interactions involving the terminal G·U pair of the P1 helix in both the *T. thermophila* and *P. carinii* ribozymes (*10*, *36*−*40*). The overall binding affinity for r(GACUC**C**) is ∼7-fold less favorable than for r(GACUCU), and the $\Delta G°_{37}$ of tertiary interactions is less favorable by 2.8 kcal/mol. Evidently, the terminal G·U pair contributes 2.8 kcal/mol in favorable free energy of tertiary interactions (Table 3). This value is similar to the value of 3 kcal/mol determined for the *T. thermophila* ribozyme (*36*, *37*, *40*) but less than the 4.3 kcal/mol for the *P. carinii* ribozyme (*10*).

Binding of Truncated 5′ Exon Mimics. Contributions of individual nucleotides to tertiary interactions were further characterized by removing nucleotides from the 5′ end of the 5′ exon mimic (Table 3). The oligonucleotides r(_ACU-CU) and r(_ _CUCU) bind to the ribozyme with K_d values of 233 and 360 nM, respectively, which are less favorable than the K_d of 6.9 nM for the full-length 5′ exon mimic,

Table 3: Binding of 5′ Exon Mimics of Varying Length and Base Composition in H10Mg Buffer at 37 °C[a]

	binding to the ribozyme		binding to r(GGAGGC)		tertiary interactions	
oligonucleotide	K_d (nM)	$-\Delta G°_{total}$[b] (kcal/mol)	K_d[b] (mM)	$-\Delta G°_{base\ pairing}$ (kcal/mol)	$-\Delta G°_{BETI}$[c] (kcal/mol)	BETI[d]
r(GACUCU)[e]	6.9 ± 0.9	11.6	(1.1)	(4.2)	7.4	159000
	3.8 ± 1[f]	11.9[f]			7.7[f]	290000[f]
r(G**C**CUCU)	0.7 ± 0.1	13.0	0.001	8.5	4.5	1500
r(G**G**CUCU)	4.0 ± 0.6	11.9	1.5	4.1	7.8	320000
r(G**U**CUCU)	0.6 ± 0.2	13.1	0.4	4.9	8.2	670000
r(_ACUCU)[e]	233 ± 27	9.4	(1.3)	(4.1)	5.3	5500
r(_**C**CUCU)	8.3 ± 2	11.5	0.07	5.9	5.6	8000
r(_**G**CUCU)[e]	58 ± 2.9	10.3	(2.9)	(3.6)	6.7	50000
r(_**U**CUCU)	380 ± 90	9.1	1.8	3.9	5.2	4700
r(_ _CUCU)	360 ± 50	9.1	(38.9)	(2.0)	7.1	110000
r(GACUC**C**)	50 ± 5	10.4	0.08	5.8	4.6	1600
r(**U**GACUCU)[e]	8.2 ± 1.2	11.5	(1.1)	(4.2)	7.3[g]	134000[g]
			(0.07)[h]	(5.9)[h]	5.6[h]	8400[h]

[a] Ribozyme binding K_d values were determined by gel retardation assays in H10Mg buffer at pH 7.5. Values in parentheses were predicted as described in Materials and Methods. Underlined bold nucleotides represent differences in the 5′ exon mimic sequence relative to r(GACUCU). [b] $\Delta G°_{total}$ is determined from the equation $\Delta G°_{37} = RT \ln(K_d)$, where $R = 0.001987$ kcal mol^{-1} K^{-1} and $T = 310$ K. [c] $\Delta G°_{BETI}$ is determined as the difference between $\Delta G°_{total}$ and $\Delta G°_{base\ pairing}$. [d] BETI is determined by dividing the K_d for base pairing by the K_d for ribozyme binding. [e] Thermodynamics for base pairing are predicted from the experimental values for r(GACUC**C**), r(_ACUC**C**), or r(_**G**CUC**C**) as described in Materials and Methods. [f] Binding to the ribozyme was assessed via a direct gel binding assay. [g] Values calculated if the 5′ U does not form an additional base pair with the intron (Figure 1), but stacks on the adjacent base pair. [h] Values calculated if the 5′ U forms an additional base pair with the intron, and oligonucleotide binding is calculated for the r(UGACUCU)·r(GGAGGCA) duplex.

Table 4: Thermodynamics for Binding to IGS Mimics in H10Mg Buffer[a]

	thermodynamics obtained from $1/T_M$ vs $\ln(C_T/4)$ plots				thermodynamics obtained from the average curve fits			
oligonucleotide	$-\Delta G°_{37}$ (kcal/mol)	$-\Delta H°$ kcal/mol)	$-\Delta S°$ (eu)	T_m[b] (°C)	$-\Delta G°_{37}$ (kcal/mol)	$-\Delta H°$ (kcal/mol)	$-\Delta S°$ (eu)	T_m[b] (°C)
Thermodynamics for Binding to r(GGAGGC)								
r(GACUC**C**)	5.77 ± 0.47	41.34 ± 6.79	114.67 ± 22.21	31.4	5.68 ± 0.46	47.11 ± 10.04	133.58 ± 33.44	31.5
r(_ACUC**C**)	5.70 ± 0.05	43.01 ± 1.97	120.29 ± 6.47	31.1	5.71 ± 0.41	47.78 ± 11.91	135.64 ± 39.31	31.8
r(G**C**CUCU)	8.51 ± 0.07	59.29 ± 2.14	163.63 ± 6.67	47.7	8.79 ± 0.49	66.35 ± 12.14	185.60 ± 37.62	47.9
r(G**C**CUC**C**)	10.69 ± 0.60	77.87 ± 10.61	216.63 ± 23.57	54.5	10.68 ± 0.62	76.99 ± 9.59	213.78 ± 29.22	54.7
r(_**C**CUCU)	5.85 ± 0.39	44.03 ± 7.89	123.97 ± 25.68	30.5	5.45 ± 0.22	49.23 ± 8.16	141.61 ± 26.93	30.4
G**C**C**dU**CU	(8.20 ± 0.10)	(73.30 ± 4.94)	(209.90 ± 15.65)	(44.2)	(8.46 ± 0.39)	(87.18 ± 11.05)	(253.80 ± 34.74)	(44.0)
G**C**CU**dC**U	8.27 ± 0.39	74.99 ± 11.17	215.12 ± 35.22	44.3	8.12 ± 0.09	69.14 ± 6.94	196.72 ± 22.52	44.3
G**C**CUC**dU**	(8.19 ± 0.80)	(62.98 ± 13.90)	(176.76 ± 43.66)	(45.4)	(8.38 ± 0.80)	(75.92 ± 9.37)	(217.77 ± 28.84)	(44.7)
d(G**C**CT**C**)rU	6.32 ± 0.59	77.73 ± 19.88	230.25 ± 63.99	36.2	6.50 ± 0.26	81.06 ± 22.15	240.40 ± 71.31	36.9
r(G**G**CUCU)	4.10 ± 0.52	54.21 ± 9.85	161.57 ± 32.10	23.7	4.08 ± 0.58	52.35 ± 9.93	155.55 ± 33.69	23.1
r(G**G**CUC**C**)	5.42 ± 0.16	34.16 ± 3.89	92.69 ± 12.89	27.2	5.25 ± 0.13	39.91 ± 1.37	111.76 ± 4.44	27.4
r(_**G**CUC**C**)	5.15 ± 0.66	45.61 ± 20.47	130.81 ± 6.33	27.2	5.04 ± 1.78	47.75 ± 11.84	137.36 ± 36.88	28.3
r(G**U**CUCU)	4.89 ± 0.16	52.14 ± 3.57	152.33 ± 11.97	27.6	4.86 ± 0.32	54.01 ± 6.56	158.47 ± 22.05	27.7
r(G**U**CUC**C**)	7.08 ± 0.14	93.29 ± 9.50	277.97 ± 30.53	38.8	7.15 ± 0.16	86.31 ± 18.53	255.23 ± 60.14	39.3
r(_**U**CUCU)	(3.94 ± 0.17)	(36.43 ± 2.76)	(104.77 ± 9.43)	(16.4)	(2.45 ± 1.08)	(57.95 ± 11.46)	(178.95 ± 40.35)	(16.6)
G**U**C**dU**CU	(5.30 ± 0.36)	(39.12 ± 5.47)	(109.07 ± 18.58)	(27.5)	(3.81 ± 0.19)	(66.97 ± 8.80)	(203.64 ± 28.66)	(24.9)
G**U**CU**dC**U	(4.75 ± 0.27)	(53.82 ± 7.81)	(158.21 ± 25.83)	(27.7)	(4.61 ± 0.13)	(62.30 ± 8.82)	(186.00 ± 28.59)	(27.7)
G**U**CUC**dU**	(5.03 ± 0.12)	(53.01 ± 2.96)	(154.71 ± 9.94)	(28.4)	(4.48 ± 0.43)	(66.36 ± 4.47)	(199.53 ± 15.03)	(27.7)
d(G**T**CT**C**)rU	2.04 ± 0.46	68.48 ± 7.48	214.22 ± 25.26	17.9	2.24 ± 0.84	62.75 ± 17.93	195.11 ± 60.43	17.1
Thermodynamics for Binding to r(GGAGUC)								
r(GACUCU)	6.69 ± 0.56	68.39 ± 15.96	198.92 ± 49.83	37.7	6.75 ± 0.13	74.41 ± 19.06	218.15 ± 61.40	37.9
dGACUCU	6.02 ± 0.03	65.17 ± 2.40	190.69 ± 7.82	34.6	6.00 ± 0.06	67.31 ± 3.49	197.68 ± 11.45	34.6
G**dA**CUCU	6.05 ± 0.22	69.76 ± 9.70	205.41 ± 31.43	34.9	6.11 ± 0.13	66.68 ± 17.44	195.31 ± 56.65	35.0
GA**dC**UCU	6.22 ± 0.31	69.67 ± 10.97	204.60 ± 35.39	35.6	6.23 ± 0.10	67.55 ± 5.85	197.73 ± 19.10	35.6
GAC**dU**CU	6.20 ± 0.01	62.76 ± 1.58	182.36 ± 5.10	35.4	6.22 ± 0.03	57.66 ± 2.56	165.86 ± 8.23	35.3
GACU**dC**U	6.32 ± 0.27	68.02 ± 10.10	189.95 ± 32.48	36.0	6.34 ± 0.09	66.89 ± 11.72	195.24 ± 38.04	36.1
GACUC**dU**	6.39 ± 0.39	62.05 ± 10.89	179.45 ± 35.05	36.3	6.39 ± 0.14	59.51 ± 7.10	171.26 ± 23.24	36.3

[a] Oligonucleotides were melted in H10Mg buffer at pH 7.5. Differences in the $\Delta H°$ of duplex formation of >15% may indicate non-two-state melting of these duplexes and are in parentheses. [b] The T_m is calculated at a strand concentration of 100 μM.

r(GACUCU). The tertiary interactions with r(_ _CUCU) are 1.8 kcal/mol more favorable than those with r(_ACUCU), however. Truncating r(G**C**CUCU) to give r(_**C**CUCU) also results in less favorable overall binding, changing the K_d from 0.7 to 8.3 nM. Comparison of the binding of r(_**C**CUCU) and r(_ _CUCU) reveals that r(_ _CUCU) has an overall weaker affinity for binding to the ribozyme, but the tertiary interactions are 1.5 kcal/mol more favorable than for r(_**C**CUCU).

Binding of Extended 5′ Exon Mimics. The binding of a 5′ exon mimic extended on the 5′ end, r(**U**GACUCU), was studied because the 5′ U has the potential of forming an additional base pair with the intron (Figure 1 and Table 3). The results in Table 3 show that the 5′ U has little effect on binding affinity; K_d values are 6.9 nM for r(GACUCU) and 8.2 nM for r(**U**GACUCU). Thus, the 5′ U does not seem to be forming an additional base pair since this would increase the binding affinity by ~15-fold (Table 3). Alternatively,

Table 5: Binding of 3′ Extended 5′ Exon Mimics in M10Mg, pH 6.5 Buffer at 37 °C and Reactivity at pH 7.5 in H10Mg Buffer[a]

oligonucleotide	$K_{d,C-10/1x}$ (nM)	$-\Delta G°_{C-10/1x}$ (kcal/mol)	$K_{d,base\ pairing}$ (mM)	$-\Delta G°_{base\ pairing}$ (kcal/mol)	$-\Delta G°_{BETI}$ (kcal/mol)	BETI	k_{cat} (min^{-1})[b]
GACUCU	26 ± 11	10.8	1.1	4.2	6.6	42000	
GACUCU**A**	32 ± 9	10.6	0.18	5.3	5.3	5600	0.12
			(0.35)	(4.9)	(5.7)	(11000)	
GACUCU**C**	9.2 ± 4	11.4	0.10	5.7	5.7	10400	0.048
			(0.93)	(4.3)	(7.1)	(101000)	
GACUCU**G**	22 ± 6	10.9	0.16	5.4	5.5	7300	0.022
			(0.35)	(4.9)	(6.0)	(16000)	
GACUCU**U**	37 ± 14	10.5	2.40	3.7	6.8	65000	0.022
			(0.93)	(4.3)	(6.2)	(25000)	
G**C**CUCU	12 ± 4	11.2	1.0×10^{-3}	8.5	2.7	83	
G**C**CUCU**C**	1.5 ± 0.5	12.5	8.5×10^{-5}	10.0	2.5	60	0.050
			(8.6×10^{-4})	(8.6)	(3.9)	(580)	
G**C**CUCU**G**	4.0 ± 2	11.9	1.5×10^{-4}	9.7	2.2	40	0.090
			(3.3×10^{-4})	(9.2)	(2.7)	(83)	

[a] Ribozyme binding affinity was measured via a direct gel binding assay at pH 6.5 to eliminate hydrolysis of the 3′ terminal nucleotide. Thermodynamics for base pairing to the IGS were calculated as described in Materials and Methods. Values in parentheses are calculated if the terminal nucleotide does not form a base pair upstream of the IGS and only stacks on the adjacent G·U pair, which is estimated from stacking on A·U pairs. It is assumed that the thermodynamics of base pairing are identical at pH 6.5 and 7.5. [b] Determined by single-turnover experiments for the pG addition reaction at pH 7.5 as described in Materials and Methods.

Table 6: Binding of Deoxy-Substituted 5′ Exon Substrates in H10Mg Buffer at 37 °C[a]

	binding to C-10/1x		binding to r(GGAGUC)	contribution of individual 2′-OHs to tertiary interactions
oligonucleotide	K_d (nM)	$-\Delta G°_{total}$ (kcal/mol)[b]	$-\Delta G°_{base\ pairing}$ (kcal/mol)	$-\Delta\Delta G°_{OH\rightarrow H\ mutation}$ (kcal/mol)[c]
GACUCU	6.9 ± 0.9	11.6	6.7	–
dGACUCU[d]	3.0 ± 0.2	12.1	6.0	−1.2
G**dA**CUCU[d]	5.0 ± 1.4	11.8	6.1	−0.9
GA**dC**CUCU[d]	9.0 ± 2.2	11.4	6.2	−0.4
GAC**dU**CU	176 ± 70	9.6	6.2	1.5
GACU**dC**U	68 ± 10	10.2	6.3	1.0
GACUC**dU**	40 ± 6	10.5	6.4	0.8
d(GACUC)rU	>8000	<7.2	–	–

[a] Ribozyme binding K_d values were determined with a competitive gel binding assay in H10Mg buffer at pH 7.5. The thermodynamics for base pairing to r(GGAGUC) were measured by optical melting. r(GGAGUC) is not the natural IGS mimic and was used to estimate the effects of deoxy substitutions on the free energy of base pairing because the r(GACUCU)·r(GGAGGC) duplex is too weak to measure. Underlined residues and "d" represent deoxy substitutions placed in the oligonucleotide. [b] $\Delta G°_{total}$ is determined from the equation $\Delta G°_{37} = RT \ln(K_d)$, where $R = 0.001987$ kcal mol^{-1} K^{-1} and $T = 310$ K. [c] $\Delta\Delta G°_{OH\rightarrow H\ mutation}$ is determined as the difference between the binding of r(GACUCU) and the deoxy-substituted oligonucleotide, correcting for differences in the $\Delta G°$ of base pairing. [d] The enhancement in tertiary binding observed when 2′-hydroxyls are removed on the 5′ end of the 5′ exon mimic may be due to the preference of deoxynucleotides for adopting a more B-form sugar pucker or due to the greater flexibility of deoxy sugars.

the additional base pair forms, but an unfavorable interaction offsets the favorable base pairing interaction.

Oligonucleotides extended on the 3′ end were also studied for binding to the ribozyme using a direct gel binding assay completed in M10Mg, pH 6.5 buffer (Table 5); this buffer was used to eliminate cleavage of the 3′ nucleotide that occurs at pH 7.5. Addition of a 3′ C to give r(GACUCU**C**) increases the binding affinity from 26 to 9.2 nM, whereas addition of a 3′ A, G, or U does not appreciably affect binding. This suggests that the increased binding affinity for r(GACUCU**C**) relative to that for r(GACUCU) at pH 6.5 may be due to formation of a G-C pair after the cleavage site (see Figure 1). If this G-C pair forms, it makes tertiary interactions less favorable by 0.9 kcal/mol (Table 5).

Recognition of 2′-Hydroxyl Groups. The contributions of 2′-hydroxyl groups to binding affinity and tertiary interactions were investigated because **d**(GACTC)rU binds much more weakly to the ribozyme than r(GACUCU), >8000 versus 6.9 nM, respectively, at pH 7.5 (Tables 3 and 6). Furthermore, tertiary interactions to 2′-hydroxyl groups have been found in forms of the *T. thermophila* intron (*41*−*49*). Results for individual deoxy substitutions suggest that the first three 2′-hydroxyl groups on the 5′ end do not form tertiary interactions with the ribozyme (Table 6). Deoxy substitution of any of the first three ribose sugars at the 3′ end, however, results in a large decrease in overall binding affinity; GAC**dU**CU, GACU**dC**U, and GACUC**dU** bind to the ribozyme with K_d values of 176, 68, and 40 nM, respectively (Table 6).

To separate the effects of deoxy substitutions on base pairing and tertiary interactions, the thermodynamics of the 5′ exon mimic DNA−RNA chimeras binding to r(5′GGAGUC3′) were measured. This duplex was used because the natural r(5′GACUCU3′)·r(3′CGGAGG5′) duplex is too unstable to measure. On average, single deoxy substitutions make the duplex less stable by 0.5 kcal/mol relative to the RNA−RNA duplex (Tables 4 and 6). Correction for the effects of individual deoxy substitutions on overall binding affinity indicates that 2′-hydroxyl groups at the −3, −2, and −1 positions contribute 1.5, 1.0, and 0.8 kcal/mol to tertiary interactions, respectively (Table 6).

Table 7: Probing the Tertiary Interactions of Non-Natural Substrates (Binding of Substituted 5′ Exon Substrates in H10Mg Buffer at 37 °C)[a]

	binding to C-10/1x		binding to the IGS mimic	contribution of modifications to tertiary interactions	
oligonucleotide	K_d (nM)	$-\Delta G°_{total}$ (kcal/mol)[b]	$-\Delta G°_{base\ pairing}$ (kcal/mol)	$-\Delta G°_{BETI}$ (kcal/mol)	$-\Delta\Delta G°_{mutation}$ (kcal/mol)[b]
G**C**CUCU	0.7 ± 0.1	13.0	8.5	4.5	−
G**C**C**dU**CU	1.6 ± 0.4	12.5	8.2	4.3	−0.2
G**C**CU**dC**U	1.9 ± 0.6	12.4	8.3	4.1	−0.4
G**C**CU**C**dU	2.2 ± 0.2	12.3	8.2	4.1	−0.4
d(G**C**CTC)rU	32 ± 3	10.6	6.3	4.3	−0.2
G**C**C**U**C**C**	3.1 ± 0.6	12.1	10.7	1.4	−3.1
G**G**CUCU	4.0 ± 0.6	11.9	4.1	7.8	−
G**G**C**dU**CU[c]	170 ± 12	9.6	∼3.6	∼6.0	∼ −1.8
G**G**CU**dC**U[c]	20 ± 2	10.9	∼3.6	∼7.3	∼ −0.5
G**G**CU**C**dU[c]	19 ± 1	10.9	∼3.6	∼7.3	∼ −0.5
d(G**G**CTC)rU[d]	8000 ± 220	7.2	∼1.2	∼6.0	∼ −1.8
G**G**C**U**C**C**	22 ± 3	10.9	5.4	5.5	−2.4
G**U**CUCU	0.6 ± 0.2	13.1	4.9	8.2	−
G**U**C**dU**CU	9.0 ± 2	11.4	5.3	6.1	−2.1
G**U**CU**dC**U	4.2 ± 0.2	11.9	4.8	7.1	−1.1
G**U**CU**C**dU	3.1 ± 0.3	12.1	5.0	7.1	−1.1
d(G**T**CTC)rU	824 ± 110	8.6	2.0	6.6	−1.6
G**U**C**U**C**C**	3.9 ± 1.0	11.9	7.1	4.8	−3.4

[a] Free energies are calculated as described in Table 1. [b] Calculated from the difference in $\Delta G°_{BETI,37}$ between the sequence of interest and the corresponding unmodified sequence. [c] Values with an ∼ sign were predicted by assuming the free energy increment for introducing a single deoxy substitution into r(G**G**CUCU) is 0.5 kcal/mol, which is the average penalty for introducing a single deoxy into the 5′GACUCU•3′CUGAGG duplex. [d] The free energy for the 5′**d**(G**G**CTC)rU•3′CGGAGG duplex was estimated by subtracting the average penalty of 2.9 kcal/mol for binding of **d**(G**T**CTC)rU and **d**(G**C**CTC)rU to the IGS mimic, relative to base pairing of the all ribo 5′ exon mimic.

Table 8: Summary of Free Energy Contributions (kcal/mol at 37 °C) to Tertiary Interactions for Various 5′ Exon Mimics[a]

tertiary interaction	GACUCU	G**C**CUCU	G**G**CUCU	G**U**CUCU
splice site G•U pair	−2.8	−3.1	−2.4	−3.4
−1 OH	−0.8	−0.4	∼ −0.5[b]	−1.1
−2 OH	−1.0	−0.4	∼ −0.5[b]	−1.1
−3 OH	−1.5	−0.2	∼ −1.8[b]	−2.1

[a] Free energies are calculated as the difference in the energies of tertiary interactions between the substituted oligonucleotide and all-ribose. [b] Considered an estimate because both the affinities of binding to the ribozyme and to IGS are estimates.

To determine if the same tertiary interactions form when the G•A pair is changed to a G•G, G•U, or G-C pair, tertiary contacts observed for r(GACUCU) were probed for r(G**G**CUCU), r(G**U**CUCU), and r(G**C**CUCU) (Table 7). Free energy increments for substitutions are summarized in Table 8. For r(GACUCU), r(G**G**CUCU), r(G**U**CUCU), and r(G**C**CUCU), changing the terminal G•U pair to a G-C pair makes tertiary interactions less favorable by essentially the same amount (Tables 3, 7, and 8). Interactions with the 2′-hydroxyl group at the −3 position of r(G**G**CUCU) and r(G**U**CUCU) contribute 1.8 and 2.1 kcal/mol of tertiary stability at 37 °C, respectively, which is similar to the value of 1.5 kcal/mol associated with this 2′-hydroxyl in r(GACUCU) (Tables 6−8). Contributions to binding of r(G**C**CUCU) from tertiary contacts with the hydroxyl group at position −3, however, are smaller than for r(GACUCU), r(G**G**CUCU), and r(G**U**CUCU). Substitution of deoxy for ribose at positions −1 and −2 of r(G**C**CUCU) has a cumulative effect smaller than that of substitution in r(GACUCU) or r(G**U**CUCU) (Tables 6−8).

Tertiary interactions with 5′ exon mimic 2′-hydroxyl groups were also measured for the *T. thermophila* ribozyme when the splice-site G•U pair was replaced with a G-C pair (*37*) and when tertiary contacts with IGS 2′-hydroxyls were disrupted (*26*). In both of these investigations, the free energy of tertiary interactions with the 2′-hydroxyl group at the −3 position is less favorable when mutations of other tertiary contacts are made. These results are similar to the data in Table 8 where the tertiary binding free energy associated with the 2′-hydroxyl group at position −3 is less favorable when the position −5 G•A pair is replaced with a G-C pair. These data suggest that there is some cooperativity between the interactions that drive docking of the P1 helix in these ribozymes.

Reactivity of Natural and Non-Natural Substrates. The effect of changing the base pair downstream of the cleavage site in the pG addition reaction was also measured (Table 5). These experiments were conducted because the *C. albicans* ribozyme has the potential of forming a base pair downstream of the cleavage site (Figure 1). Such base pairs may be important for catalysis because they may dictate the shape of the phosphodiester bond that is broken in the first step of self-splicing. In each case, however, the nucleotide downstream of the cleavage site had only a modest effect on k_{cat}.

DISCUSSION

Two group I intron model systems were cloned from the LSU rRNA gene of *C. albicans* (Figure 1). One construct contains the intron and truncated 5′ and 3′ exons. The second construct is a ribozyme that lacks 10 nucleotides on the 5′ end and one nucleotide on the 3′ end of the intron. These systems were used to study the reactivity of the truncated precursor and ribozyme (Tables 1 and 2 and Figures 2 and 3) and to determine the factors that affect binding of 5′ exon mimic substrates to the ribozyme (Figure 5 and Tables 3 and 5−8).

Precursor and Ribozyme Kinetics. The C-h precursor self-splices in H10Mg (10 mM Mg^{2+}) buffer (Table 1 and Figure

2). The reaction rate as a function of pG concentration fits the Michaelis−Menten equation, and the parameters are similar to those measured for the *T. thermophila* precursor (*35*) (Table 1).

The C-10/lx ribozyme catalyzes oligonucleotide exon ligation (*50*), pG addition (*21*), and hydrolysis (*20*) reactions (Table 2 and Figure 3). Kinetic parameters for pG addition, determined by steady-state kinetics, and for hydrolysis, determined by single-turnover experiments, are similar to parameters determined for the *T. thermophila* ribozyme (*20*). Evidently, the C-h precursor and C10/1x ribozyme do not require exogenous factors for folding into their active conformations.

Binding of Extended Oligonucleotides. The oligonucleotide extended on the 5′ end with a U, r(**U**GACUCU), which has the potential of forming an additional base pair with the intron, binds similarly as the natural 5′ exon mimic, r(GACUCU), 8.2 versus 6.9 nM, respectively (Table 3). These results suggest that the 5′ U does not form an additional base pair when bound to the ribozyme or the base pair forms, but this favorable interaction is offset by unfavorable interactions.

The 5′ exon mimic was also extended on the 3′ end, with the level of binding measured at pH 6.5 to minimize hydrolysis of the 3′ nucleotide (Table 5). For r(GACUCU**C**), which has the potential of forming an additional base pair with the ribozyme, the K_d is 9.2 nM, compared with 26 nM for r(GACUCU). In contrast, adding A, G, or U to the 3′ end does not appreciably change the binding affinity relative to that of r(GACUCU). This suggests that the terminal C in r(GACUCU**C**) may form the potential G-C base pair at the end of the P1 helix (Figure 1). Formation of this G-C pair, however, is expected to strengthen binding by roughly 11-fold (*30*, *31*), not the 2.5-fold that was measured. That is, the free energy of tertiary interactions is less favorable by 0.9 kcal/mol when the 3′ C is added. These results are consistent with the formation of unfavorable interactions with the 3′ C. For the *T. thermophila* ribozyme, adding a single A after the cleavage site makes binding of the substrate less favorable by 3−40-fold (*51*, *52*). For that ribozyme, there is no nucleotide to base pair with the A after the cleavage site. Our results suggest that formation of a base pair after the cleavage site may compensate for the unfavorable interactions associated with a nucleotide 3′ of the cleavage site.

Role of the G·U Pair at the Splice Junction. For the *T. thermophila* (*36*−*40*) and *P. carinii* (*10*) ribozymes, changing the G·U pair at the splice junction to a G-C pair makes tertiary interactions less favorable by 3 and 4.3 kcal/mol, respectively. For the *C. albicans* ribozyme, changing the G·U pair to a G-C pair makes tertiary interactions less favorable by 2.8 kcal/mol (Table 3). Thus, the interactions with the G·U pair in the *C. albicans* ribozyme appear to be more like those in *T. thermophila* than those in *P. carinii*. With *T. thermophila*, the G·U to G-C change prevents the exocyclic amine from forming tertiary contacts (*40*), and the effect is presumably primarily responsible for the changes seen with the *P. carinii* and *C. albicans* ribozymes.

The J4/5 internal loop of group I introns is the region where tertiary contacts form to the exocyclic amino of the G·U pair present at the splice site (*39*). Interestingly, the thermodynamic stabilities of the J4/5 loops in the *T. thermophila* and the *C. albicans* ribozymes are similar, $\Delta G^\circ_{37,loop}$ values of 3.2 and 3.5 kcal/mol (*53*), respectively. The J4/5 loop in *P. carinii*, however, is more stable, with a $\Delta G^\circ_{37,loop}$ of 1.9 kcal/mol (*53*). Thus, the thermodynamic stabilities of these loops correlate with changes in the free energy of tertiary interactions for the G·U to G-C substitution. The results suggest that the *P. carinii* J4/5 loop may be more preorganized to accept tertiary interactions than either the *T. thermophila* or *C. albicans* loops.

Role of the G·A Pair As Revealed by Base Pair Substitutions. To determine the contribution to overall binding affinity and tertiary interactions of the G·A pair at position −5 in the P1 helix (Figure 1), it was replaced with G·G, G·U, and G-C pairs (Table 3 and Figure 5). The overall binding affinities of r(GACUCU), r(G**G**CUCU), r(G**U**CUCU), and r(G**C**CUCU) show that stability depends on pairing at the −5 position in the following order: G·A = G·G < G−C = G·U (Table 3). Comparison of the contributions that base pairing and tertiary interactions make in binding of these substrates provides insight into how the ribozyme recognizes its 5′ exon substrate. The oligonucleotide with a G-C pair, r(G**C**CUCU), binds more tightly to the ribozyme than r(GACUCU), but exhibits a much less favorable tertiary binding free energy, −4.5 versus −7.4 kcal/mol, respectively. The oligonucleotide with the G·U pair, however, binds most tightly to the ribozyme and exhibits a tertiary binding free energy similar to that of the oligonucleotides with G·A or G·G pairs, −8.2 versus −7.4 and −7.8 kcal/mol, respectively (Table 3). Thus, the tighter binding exhibited with r(G**U**CUCU), when compared to that with r(GACUCU), is due to its ability to base pair more tightly to the ribozyme while maintaining a similar tertiary binding affinity.

The *T. thermophila* ribozyme forms a G·U pair at the −5 position when bound to the natural substrate (see secondary structure in ref *54*). Previous experiments have investigated the effects of changing this G·U pair to a G-C pair and suggest that the G·U pair modestly contributes to tertiary binding of substrate; changing the G·U pair to a G-C pair makes the tertiary binding free energy less favorable by ∼1.2 kcal/mol at 42 °C (*37*). For the *C. albicans* ribozyme, however, the energetic cost to tertiary binding free energy of changing the G·A pair to a G-C pair is much larger, 2.9 kcal/mol at 37 °C (Table 3). The large difference in the free energy of tertiary interactions mediated by these two non-Watson−Crick pairs may be a means of compensating for the less favorable base pairing of duplexes containing a G·A (*55*) versus a G·U pair (*31*, *56*), and suggests that tertiary interactions mediated at the −5 position may be different between the two ribozymes.

Binding of 5′-Truncated Oligonucleotides. Previous studies with the *T. thermophila* and *P. carinii* ribozymes have shown that eliminating as many as two nucleotides on the 5′ end of a 5′ exon mimic has no effect on tertiary binding of the substrate (*10*, *57*, *58*). For the *C. albicans* ribozyme, however, the free energy contribution due to tertiary interactions changes when nucleotides are eliminated from the 5′ end of 5′ exon mimics (Table 3). For example, r(GACUCU) and r(_ACUCU) have tertiary free energies of −7.4 and −5.3 kcal/mol, respectively. Removing the 5′ terminal G from r(G**G**CUCU) and r(G**U**CUCU) also makes the free energy of tertiary interactions less favorable, so the effect is general when there is a non-Watson−Crick pair at the −5 position.

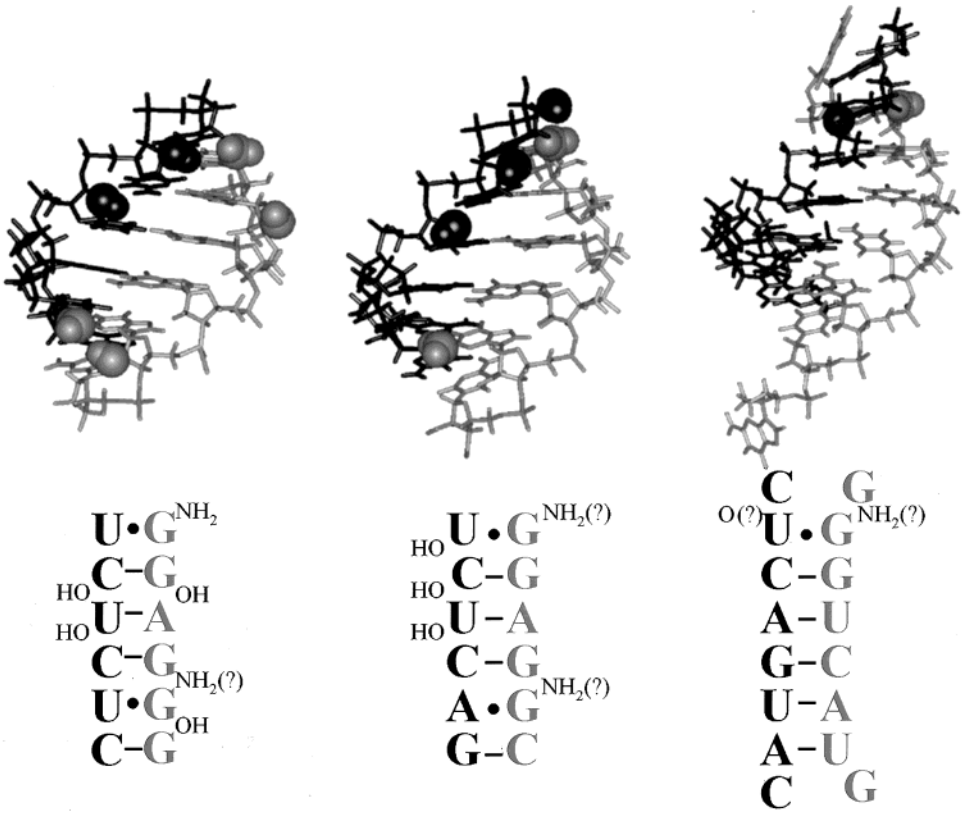

FIGURE 6: Models of the 5′ exon substrate bound to the IGS in (from left to right) the *T. thermophila* (*26*, *37*, *38*, *40*, *41*, *43*, *44*), *C. albicans*, and *P. carinii* (*6*, *8*, *10*) group I introns. Space-filling atoms are used for functional groups that are thought to form tertiary interactions when the P1 helix is docked into the catalytic core. Gray strands are internal guide sequences and black strands the 5′ exons, with the 3′ end at the top. Note that the tertiary interactions to IGS strand 2′-hydroxyls were not probed for the *P. carinii* or *C. albicans* ribozymes. The question marks denote tertiary interactions for which there is only circumstantial evidence. The NH_2 groups in the terminal G·U pairs for the *P. carinii* and *C. albicans* ribozymes are likely to form tertiary interactions similar to those of *T. thermophila* (*39*, *40*, *62*). Since G·A, G·G, and G·U pairs can all form structures that present a G amino group in the minor groove (*63*), it is possible that the tertiary interactions at the −5 position also involve the amino group of G. Less favorable tertiary interactions with a terminal G·4-thioU or G·2-thioU pair formed with the *P. carinii* ribozyme suggest possible tertiary interactions with O4 and/or O2 of U (*8*).

The less favorable tertiary binding of pentamers versus hexamers suggests that the tertiary interactions are sensitive to whether a non-Watson−Crick pair is at the penultimate or terminal position in the P1 helix. NMR structures of tandem G·A and G·U pairs show that the structures are sensitive to the adjacent base pairs (*59*−*61*). Structures may also depend on whether a pair is in a terminal or penultimate position in a helix. Alternatively or in addition, the data may reflect a tertiary interaction with the terminal G-C pair.

Truncation of r(G**C**CUCU) to yield r(_**C**CUCU) and r(_ _CUCU) also changes the free energy of tertiary interactions, giving values of −4.5, −5.6, and −7.1 kcal/mol, respectively. These data can also be explained by a site set up for a tertiary interaction with the natural G·A pair. The order of tertiary binding [r(_ _CUCU) > r(_**C**CUCU) > r(G**C**CUCU)] may be the result of freeing functional groups to form the tertiary interactions normally made by the G·A pair at position −5 (Figure 1).

Role of 2′-Hydroxyl Groups for Various 5′ Exon Mimics. The K_d for **d**(GACTC)rU binding to ribozyme is >8000 nM, which is much higher than the value of 6.9 nM for r(GACUCU) (Table 6). The results of single deoxy substitutions introduced into r(GACUCU) indicate that the 2′-hydroxyl groups at the −3, −2, and −1 positions contribute 1.5, 1.0, and 0.8 kcal/mol, respectively, to tertiary interactions with the ribozyme (Table 6).

In the *T. thermophila* system, 2′-hydroxyl groups also form tertiary interactions (*26*, *41*−*46*, *48*, *49*). The interactions with the 5′ exon involve 2′-hydroxyls at the −3 and −2 positions (*41*−*43*), and they each contribute ∼0.9 kcal/mol to tertiary binding, which is similar to the tertiary contribution that each of the 2′-hydroxyl groups make in the *C. albicans* system. A tertiary contact at the −1 position is not present in the ground state of *T. thermophila*, but is implicated in the transition state (*45*, *48*, *49*).

To determine if differences in tertiary binding affinity between substrates differing at the −5 position are due to loss of specific tertiary contacts, we probed the effects of removing elements that are known to form tertiary interactions in r(GACUCU) (Tables 3 and 6−8 and Figure 6). Comparisons of the tertiary component of binding free energies when the terminal G·U pair is changed to a G-C pair indicate that the free energy of tertiary interactions with the G·U pair at the splice site are similar for r(GACUCU), r(G**G**CUCU), r(G**U**CUCU), and r(G**C**CUCU). In contrast, the tertiary contact mediated by the 2′-hydroxyl at the −3 position of r(G**C**CUCU) is energetically less favorable than that for r(GACUCU), r(G**G**CUCU), or r(G**U**CUCU), 0.2 kcal/mol versus 1.5, 1.8, and 2.1 kcal/mol, respectively (Tables 6−8). These data suggest that the 2.9 kcal/mol loss in tertiary binding free energy of r(G**C**CUCU) compared to that of r(GACUCU) may partially be due to loss of a specific

tertiary contact with the 2′-hydroxyl at the −3 position. Presumably, tertiary contacts to the G·A, G·G, or G·U pair at the −5 position align the P1 helix in a manner that allows tertiary interactions to occur to the 2′-hydroxyl group at position −3.

Summary. A *C. albicans* group I intron ribozyme and truncated precursor have been cloned. Both constructs are active as determined by in vitro assays. With the r(GACUCU) substrate, the *C. albicans* ribozyme makes tertiary contacts with three 2′-hydroxyl groups, the G·U pair formed at the splice junction, and the G·A pair formed at the −5 position of P1 (Figure 6). When the 5′ exon mimic substrate is r(G**C**CUCU), tertiary interactions to 2′-hydroxyl groups are significantly weakened, suggesting that the presence of a non-Watson−Crick base pair at the −5 position is critical for positioning of 2′-hydroxyl groups involved in tertiary interactions. Comparison of the positions and magnitudes of tertiary interactions identified in *T. thermophila*, *C. albicans*, and *P. carinii* ribozymes indicates that molecular recognition of the P1 helix differs in each case (Figure 6). The tertiary interactions may be exploited to rationally design oligonucleotide-based therapeutics to specifically target and inhibit self-splicing of group I introns. Since *C. albicans* is easily grown in cell culture, it provides an opportunity for in vivo testing of binding enhancement by tertiary interactions (*6*−*8*, *10*, *11*) and inhibition of precursor self-splicing by suicide inhibition as therapeutic strategies for targeting RNA (*9*).

NOTE ADDED IN PROOF

Preliminary assays with a semisynthetic ribozyme with the G·A pair at the −5 position of P1 replaced with an inosine·A pair suggest that the amino group of G forms a tertiary interaction as suggested in Figure 6.

ACKNOWLEDGMENT

We thank Dr. Frank Gigliotti and Wendy Watson for providing *C. albicans* clinical isolates, Susan Schroeder for providing unpublished data on the thermodynamics of the J4/5 internal loops, and Jess Childs for suggesting binding experiments on r(G**U**CUCU) and critical reading of the manuscript.

REFERENCES

1. Schaberg, D. R., Culver, D. H., and Gaynes, R. P. (1991) *Am. J. Med. 91*, 72S−75S.
2. Sternberg, S. (1994) *Science 266*, 1632−1634.
3. Miletti, K. E., and Leibowitz, M. J. (2000) *Antimicrob. Agents Chemother. 44*, 958−966.
4. Mei, H. Y., Cui, M., Lemrow, S. M., and Czarnik, A. W. (1997) *Bioorg. Med. Chem. 5*, 1185−1195.
5. Mercure, S., Montplaisir, S., and Lemay, G. (1993) *Nucleic Acids Res. 21*, 6020−6027.
6. Testa, S. M., Haidaris, C. G., Gigliotti, F., and Turner, D. H. (1997) *Biochemistry 36*, 15303−15314.
7. Testa, S. M., Gryaznov, S. M., and Turner, D. H. (1998) *Biochemistry 37*, 9379−9385.
8. Testa, S. M., Disney, M. D., Turner, D. H., and Kierzek, R. (1999) *Biochemistry 38*, 16655−16662.
9. Testa, S. M., Gryaznov, S. M., and Turner, D. H. (1999) *Proc. Natl. Acad. Sci. U.S.A. 96*, 2734−2739.
10. Disney, M. D., Gryaznov, S. M., and Turner, D. H. (2000) *Biochemistry 39*, 14269−14278.
11. Disney, M. D., Testa, S. M., and Turner, D. H. (2000) *Biochemistry 39*, 6991−7000.
12. Merali, S., Frevert, U., Williams, J. H., Chin, K., Bryan, R., and Clarkson, A. B., Jr. (1999) *Proc. Natl. Acad. Sci. U.S.A. 96*, 2402−2407.
13. Matteucci, M. D., and Caruthers, M. H. (1980) *Tetrahedron Lett. 21*, 719−722.
14. Ogilvie, K. K., Usman, N., Nicoghosian, K., and Cedergren, R. J. (1988) *Proc. Natl. Acad. Sci. U.S.A. 85*, 5764−5768.
15. Stawinski, J., Stromberg, R., Thelin, M., and Westman, E. (1988) *Nucleic Acids Res. 16*, 9285−9298.
16. Wincott, F., DiRenzo, A., Shaffer, C., Grimm, S., Tracz, D., Workman, C., Sweedler, D., Gonzalez, C., Scaringe, S., and Usman, N. (1995) *Nucleic Acids Res. 23*, 2677−2684.
17. Mercure, S., Rougeau, N., Montplaisir, S., and Lemay, G. (1993) *Nucleic Acids Res. 21*, 1490.
18. Sambrook, J., Fritsch, E. F., and Maniatis, T. (1989) *Molecular Cloning: A Laboratory Manual*, 2nd ed., Cold Spring Harbor Laboratory Press, Cold Spring Harbor, NY.
19. Puglisi, J. D., and Tinoco, I., Jr. (1989) *Methods Enzymol. 180*, 304−325.
20. Herschlag, D., and Cech, T. R. (1990) *Biochemistry 29*, 10159−10171.
21. Zaug, A. J., Been, M. D., and Cech, T. R. (1986) *Nature 324*, 429−433.
22. Zaug, A. J., and Cech, T. R. (1986) *Science 231*, 470−475.
23. Fersht, A. (1985) *Enzyme Structure and Mechanism*, 2nd ed., W. H. Freeman, New York.
24. Bevilacqua, P. C., Sugimoto, N., and Turner, D. H. (1996) *Biochemistry 35*, 648−658.
25. Szewczak, A. A., Ortoleva-Donnelly, L., Zivarts, M. V., Oyelere, A. K., Kazantsev, A. V., and Strobel, S. A. (1999) *Proc. Natl. Acad. Sci. U.S.A. 96*, 11183−11188.
26. Strobel, S. A., and Cech, T. R. (1993) *Biochemistry 32*, 13593−13604.
27. Lin, S., and Riggs, A. R. (1972) *J. Mol. Biol. 72*, 671−690.
28. Weeks, K. M., and Crothers, D. M. (1992) *Biochemistry 31*, 10281−10287.
29. Turner, D. H. (2000) in *Nucleic Acids: Structures, Properties, and Functions* (Bloomfeild, V. A., Crothers, D. M., and Tinoco, I., Jr., Eds.) Chapter 8, University Science Books, Sausalito, CA.
30. Xia, T., SantaLucia, J., Jr., Burkard, M. E., Kierzek, R., Schroeder, S. J., Jiao, X., Cox, C., and Turner, D. H. (1998) *Biochemistry 37*, 14719−14735.
31. Mathews, D. H., Sabina, J., Zuker, M., and Turner, D. H. (1999) *J. Mol. Biol. 288*, 911−940.
32. Freier, S. M., Kierzek, R., Caruthers, M. H., Neilson, T., and Turner, D. H. (1986) *Biochemistry 25*, 3209−3213.
33. McDowell, J. A., and Turner, D. H. (1996) *Biochemistry 35*, 14077−14089.
34. Longfellow, C. E., Kierzek, R., and Turner, D. H. (1990) *Biochemistry 29*, 278−285.
35. Bass, B. L., and Cech, T. R. (1984) *Nature 308*, 820−826.
36. Knitt, D. S., Narlikar, G. J., and Herschlag, D. (1994) *Biochemistry 33*, 13864−13879.
37. Pyle, A. M., Moran, S., Strobel, S. A., Chapman, T., Turner, D. H., and Cech, T. R. (1994) *Biochemistry 33*, 13856−13863.
38. Strobel, S. A., and Cech, T. R. (1996) *Biochemistry 35*, 1201−1211.
39. Strobel, S. A., and Ortoleva-Donnelly, L. (1999) *Chem. Biol. 6*, 153−165.
40. Strobel, S. A., and Cech, T. R. (1995) *Science 267*, 675−679.
41. Bevilacqua, P. C., and Turner, D. H. (1991) *Biochemistry 30*, 10632−10640.
42. Sugimoto, N., Tomka, M., Kierzek, R., Bevilacqua, P. C., and Turner, D. H. (1989) *Nucleic Acids Res. 17*, 355−371.
43. Pyle, A. M., and Cech, T. R. (1991) *Nature 350*, 628−631.
44. Pyle, A. M., Murphy, F. L., and Cech, T. R. (1992) *Nature 358*, 123−128.
45. Herschlag, D., and Cech, T. R. (1990) *Nature 344*, 405−409.

46. Narlikar, G. J., Khosla, M., Usman, N., and Herschlag, D. (1997) *Biochemistry 36*, 2465−2477.
47. Narlikar, G. J., and Herschlag, D. (1998) *Biochemistry 37*, 9902−9911.
48. Herschlag, D., Eckstein, F., and Cech, T. R. (1993) *Biochemistry 32*, 8299−8311.
49. Herschlag, D., Eckstein, F., and Cech, T. R. (1993) *Biochemistry 32*, 8312−8321.
50. Zaug, A. J., and Cech, T. R. (1986) *Biochemistry 25*, 4478−4482.
51. Narlikar, G. J., Gopalakrishnan, V., McConnell, T. S., Usman, N., and Herschlag, D. (1995) *Proc. Natl. Acad. Sci. U.S.A. 92*, 3668−3672.
52. Bevilacqua, P. C., Li, Y., and Turner, D. H. (1994) *Biochemistry 33*, 11340−11348.
53. Schroeder, S. J., and Turner, D. H. (2001) submitted for publication.
54. Cech, T. R., Damberger, S. H., and Gutell, R. R. (1994) *Nat. Struct. Biol. 1*, 273−280.
55. Kierzek, R., Burkard, M. E., and Turner, D. H. (1999) *Biochemistry 38*, 14214−14223.
56. He, L., Kierzek, R., SantaLucia, J., Jr., Walter, A. E., and Turner, D. H. (1991) *Biochemistry 30*, 11124−11132.
57. Narlikar, G. J., Bartley, L. E., Khosla, M., and Herschlag, D. (1999) *Biochemistry 38*, 14192−14204.
58. Narlikar, G. J., Bartley, L. E., and Herschlag, D. (2000) *Biochemistry 39*, 6183−6189.
59. Wu, M., and Turner, D. H. (1996) *Biochemistry 35*, 9677−9689.
60. SantaLucia, J., Jr., and Turner, D. H. (1993) *Biochemistry 32*, 12612−12623.
61. Chen, X., McDowell, J. A., Kierzek, R., Krugh, T. R., and Turner, D. H. (2000) *Biochemistry 39*, 8970−8982.
62. Strobel, S. A., and Shetty, K. (1997) *Proc. Natl. Acad. Sci. U.S.A. 94*, 2903−2908.
63. Burkard, M. T., Turner, D. H., and Tinoco, I., Jr. (1999) in *The RNA World* (R. F. Gesteland, T. R. Cech, and J. F. Atkins, Eds.) 2nd ed., Appendix 1, pp 675−680, Cold Spring Harbor Laboratory Press, Cold Spring Harbor, NY.

BI002008R